land

MDPI

Article

Development and Application of an Environmental Vulnerability Index (EVI) for Identifying Priority Restoration Areas in the São Francisco River Basin, Brazil

Clívia Dias Coelho [1,*], Demetrius David da Silva [2], Ricardo Santos Silva Amorim [2], Bruno Nery Fernandes Vasconcelos [3], Ernani Lopes Possato [4], Elpídio Inácio Fernandes Filho [3], Pedro Christo Brandão [3], José Ambrósio Ferreira Neto [5] and Lucas Vieira Silva [3]

[1] Department of Technology in Civil Engineering, Computing, Automation, Telematics and Humanities, Campus Alto Paraopeba, Federal University of São João Del-Rei, Ouro Branco 36301-160, MG, Brazil

[2] Department of Agricultural Engineering, Campus Universitário, Federal University of Viçosa, Viçosa 36301-160, MG, Brazil; demetrius@ufv.br (D.D.d.S.); rsamorim@ufv.br (R.S.S.A.)

[3] Department of Soils, Campus Universitário, Federal University of Viçosa, Viçosa 36301-160, MG, Brazil; brunonery@ufv.br (B.N.F.V.); elpidio@ufv.br (E.I.F.F.); pedrocbrandao@gmail.com (P.C.B.); lucas.v.vieira@ufv.br (L.V.S.)

[4] Department of Forestry Engineering, Campus Universitário, Federal University of Viçosa, Viçosa 36301-160, MG, Brazil; ernani.possato@ufv.br

[5] Department of Rural Economy, Campus Universitário, Federal University of Viçosa, Viçosa 36301-160, MG, Brazil; ambrosio@ufv.br

* Correspondence: clivia.coelho@gmail.com or clivia.coelho@ufsj.edu.br

check for updates

Citation: Coelho, C.D.; da Silva, D.D.; Amorim, R.S.S.; Vasconcelos, B.N.F.; Possato, E.L.; Filho, E.I.F.; Brandão, P.C.; Ferreira Neto, J.A.; Silva, L.V. Development and Application of an Environmental Vulnerability Index (EVI) for Identifying Priority Restoration Areas in the São Francisco River Basin, Brazil. *Land* **2024**, *13*, 1475. https://doi.org/10.3390/land13091475

Academic Editors: Carla Sofia Santos Ferreira and Kristina Potočki

Received: 31 July 2024
Revised: 6 September 2024
Accepted: 10 September 2024
Published: 12 September 2024

Abstract: The environmental vulnerability diagnosis of a river basin depends on a holistic analysis of its environmental aspects and degradation factors. Based on this diagnosis, the definition of priority areas where interventions for environmental recovery should be carried out is fundamental, since financial and natural resources are limited. In this study, we developed a methodology to assess these fragilities using an environmental vulnerability index (EVI) that combines physical and environmental indicators related to the natural sensitivity of ecosystems and their exposure to anthropogenic factors. The developed EVI was applied to the headwater region of the São Francisco River Basin (SFRB), Brazil. The proposed index was based on the AHP multicriteria analysis and was adapted to include four variables representative of the study area: Land Use Adequacy, Burned Area, Erosion Susceptibility, and quantitative water balance. The EVI analysis highlighted that the presence of easily erodible soils, associated with sloping areas and land use above their capacity, generate the most vulnerable areas in the headwaters of the SFRB. The highest EVI values are primarily linked to regions with shallow, easily erodible soils like Leptosols and Cambisols, found in steep areas predominantly used for pasture. In the SFBR, the greatest vulnerability was observed within a 5 km buffer around conservation units, covering approximately 32.4% of the total area. The results of this study indicate where resources should be applied for environmental preservation in the basin under study, directing the allocation of efforts to areas with lower resilience to maintain ecosystem services.

Keywords: multicriteria analysis; GIS; land use adequacy; burned area; erosion susceptibility; water balance

1. Introduction

The conversion of soil cover through the exploitation of natural resources for the implementation of intensive and extensive farming systems has led to the fragmentation of natural environments and degradation processes over the last few decades [1,2]. The negative repercussions of this degradation, especially in areas where use was not aligned with their capabilities, include a reduction in the diversity of flora and fauna, reduction in the quantity and quality of water, and intensification of erosion processes. These impacts can be severe, depending on the resilience of the environment (inversely related to vulnerability), which reflects its capacity to absorb disturbances and maintain its structure [1,2].

To reverse degradation in rural environments, it is essential to implement actions to restore natural environments or mitigate impacts, such as the use of soil and water conservation techniques in cultivated areas. However, there is a gap between the total area that can benefit from these actions and the resources available for this purpose. It is, therefore, crucial to use territorial intelligence analysis tools to identify vulnerable areas where the implementation of recovery or mitigation actions will enable the greatest preservation and, consequently, the greatest potential for maintaining or increasing desirable ecosystem services.

Environmental assessments can be obtained by mapping potential environmental vulnerability, which indicates the susceptibility of natural spaces to the occurrence of natural or induced degradation processes. Models of analysis of environmental vulnerability use simultaneous criteria (indicators) of the analyzed area, which are represented by layers of geographic data in the Geographic Information System (GIS) environment. Usually, a multidisciplinary team supports these analyses [3–8].

In addition, due to the complexity, nonlinearity, and multiplicity of the dynamics of natural systems, the development of sufficiently general indicators of environmental vulnerability may not be realizable [1,9]. Rather, the environmental vulnerability development of indicators should be conducted at smaller scales and must be specific to the geographic and temporal context. In addition, knowing how to correctly convert data from multiple sources, such as climate, land use and cover, soils, and geomorphology properties, into an integrated assessment index is also a vital step for vulnerability assessment.

Several studies have shown that environmental vulnerability can be linked to various factors such as soil condition, terrain, vegetation, climate, and social economy [2,9–12]. However, there is no consensus on which variables should be used to establish the environmental vulnerability index for all sites, and in most cases, the choice of variables is made through a specific assessment of local physical and environmental characteristics. Choosing variables to represent vulnerability requires a careful and systematic process. The variables should have theoretical relevance based on an understanding of the factors constituting vulnerability, such as exposure to risks and capacity for recovery. On the other hand, it is essential to ensure that the variables have available, high-quality, and spatially consistent data for the entire study area.

The assessment of environmental vulnerability in a river basin is fundamental to its management, as it allows the identification of areas or resources at risk and the threats posed by the diminution or loss of such resources [13]. The study of environmental vulnerability can provide crucial information so that decision-makers can prioritize areas for the allocation of financial resources to implement alternative measures to reduce this vulnerability [14]. Given these considerations, this study aims to propose an environmental vulnerability index (IVA), considering significant geospatial variables, for application in the headwaters region of the São Francisco River Basin (SFRB), Brazil, to map areas for environmental recovery.

2. Materials and Methods

2.1. Study Area

The São Francisco River is one of the most important rivers in Brazil, with a length of 2863 km and a drainage basin covering an area of more than 639,219 km^2, corresponding to 8% of the Brazilian territory. It runs from the state of Minas Gerais, where the river rises in the Serra da Canastra Mountain range, to the Atlantic Ocean, where it flows into the border between the states of Alagoas and Sergipe [15]. The basin's drainage area covers the Northeast and Southeast regions of the country, covering 505 municipalities in six states.

This aspect reinforces the importance of this basin for the country, given that the southeast region is the most populous in Brazil, and the Northeast is the only region with a semi-arid climate, creating a significant demand for water resources from this watershed. In addition, the region is currently under significant threat from climatic effects and intensification of land use [12,16,17]. In the last decade, from October 2012 to March 2021, severe drought conditions have been recorded, affecting agricultural production and reducing the reservoir level to a critical volume of 15% [18,19].

For this study, an important area of 38,733.29 km^2 was selected, which includes three sub-basins of the headwaters of the São Francisco River: the Paraopeba River sub-basin (12,191.07 km^2), the Pará River sub-basin (12,095.23 km^2) and the sub-basin of the initial section of the São Francisco River (São Francisco 01) (14,446.99 km^2) (Figure 1).

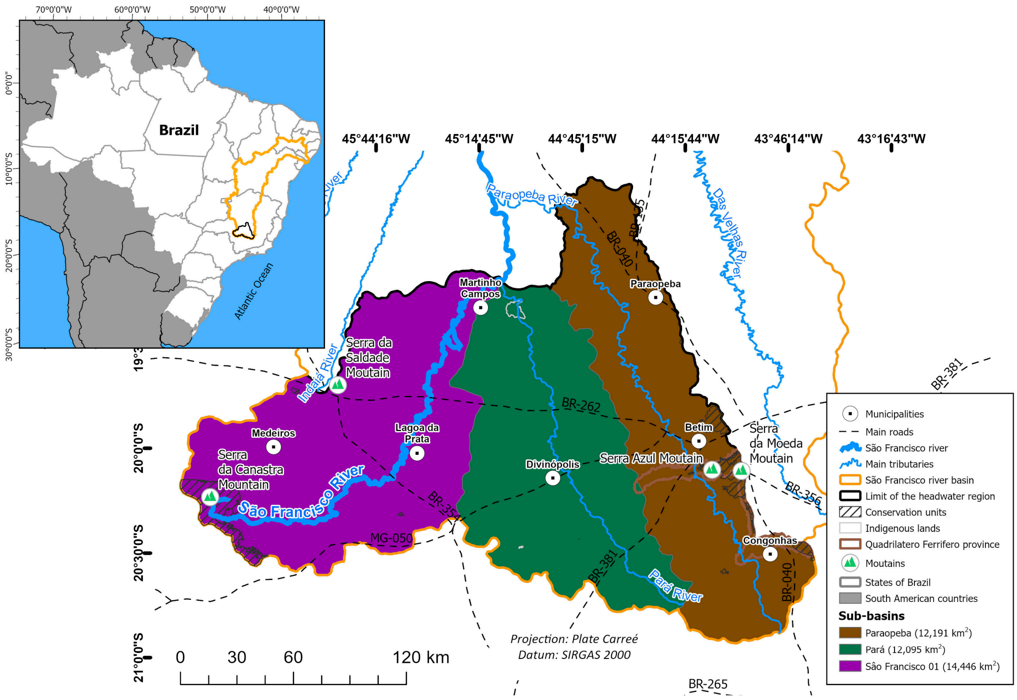

Figure 1. Study area: selected sub-basins in the headwaters of the São Francisco River Basin.

In addition, the headwaters of the SFRB have significant portions of the area in the domains of the Cerrado biome (69%) and Atlantic Forest (31%). The predominance of these two biomes was another important aspect in the selection of the area for the present study, as the Cerrado is currently the most intensely altered domain due to anthropogenic actions, while the Atlantic Forest has historically been the most altered since the colonial periods. Therefore, it is of utmost importance to conduct studies that optimize environmental restoration processes in these two morphoclimatic domains [20]. The predominant climate in the study area, according to the Koppen classification, is the Tropical Savanna (Aw), mainly in the northern region, where the Cerrado biome prevails.

In the southern region, humid subtropical (Cwa) and subtropical highland (Cwb) climates prevail in areas that coincide with the Atlantic Forest biome [21]. The average annual precipitation in the headwaters of the SFRB varied between 1135.6 and 1734.4 mm per year [22], and the annual mean temperature was 21.8 °C [23] during the period from 2001 to 2020.

In terms of soil class, most of the study area is covered by Ferralsols (47%), which are well-developed soils with a good effective depth, high total porosity, and a strong degree of structural development. However, a large part of the basin is covered by Cambisols (34%), which are poorly developed soils, often covered by a gravelly floor on the surface, and which develop pronounced surface sealing [24]. The most representative land use in the study area is agriculture and livestock (70.9%), with emphasis on corn, soybeans, sugar cane, and coffee crops, followed by natural formations (25.8%), urban areas (2.7%), and water bodies (0.6%) [25].

2.2. Environmental Vulnerability Index (EVI)

Based on the literature, the available database, and the region's soil and climate conditions, four variables were selected as the main criteria for defining environmental vulnerability in the study area: Land Use Adequacy, Burned Area, Erosion Susceptibility and quantitative water balance. The flowchart in Figure 2 presents the steps for estimating the environmental vulnerability index in the headwaters of the SFRB.

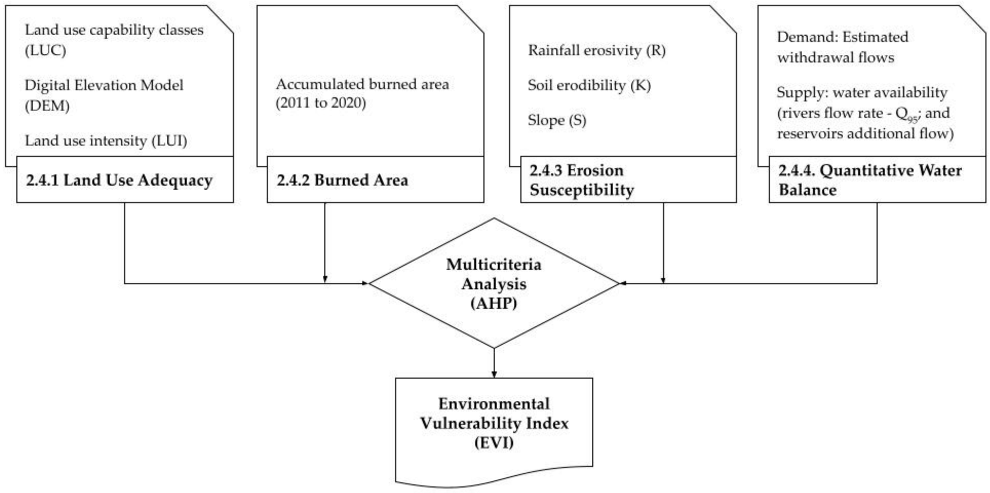

Figure 2. Steps to create the environmental vulnerability index (EVI).

Each variable was represented by a spatial thematic layer derived from satellite images, official spatial data, or data adapted by the authors. For the decision analysis, the values and classes of all maps were rescaled from 0 to 1 using a linear function. In this way, the cells on a map with high environmental vulnerability were assigned standardized values close to 1, and the cells corresponding to the least vulnerable areas were assigned standardized values close to 0.

After standardization, the relative importance (final weights) of the criteria was obtained using the Analytical Hierarchy Process (AHP), and the maps of these criteria were multiplied in a GIS environment to obtain the final EVI map. Below is a description of the data sources and analysis procedures for each of the variables used as criteria for defining the environmental vulnerability index. The raster data were derived from satellite images with a spatial resolution of 30 m, and the vector data were derived from mappings at a scale of 1:250,000; in this case, a resampling process was conducted to unify the pixel size at 30 m.

This work was carried out using databases and secondary information made available by official national agencies and research institutions (e.g., the Brazilian Institute of Geography and Statistics—IBGE, the Brazilian Agricultural Research Corporation—EMBRAPA, and the National Institute for Space Research—INPE) and international organizations (e.g., the National Aeronautics and Space Administration—NASA and the European Space Agency—ESA). It should be noted that the databases considered in this work are widely used in studies aimed at understanding the spatial behavior of different natural phenomena.

2.3. Multicriteria Analysis AHP

The analytical hierarchical process (AHP) is a multi-perspective and multi-objective decision-making model that enables users and planners to quantitatively derive a scale of preference drawn from a set of alternatives [26]. In this way, experts can convert subjective judgments into objective measures [27].

The relative significance for each individual layer is resolved with Saaty's 1–9 scale (Table 1), in which a score of 1 represents equal importance between the two variables, and a score of 9 shows the extreme importance of one variable in contrast to the other [15]. The

Saaty scale is used to define the variables using their ranking scale and priority, which helps organize them in hierarchical order through a pairwise comparison matrix.

Table 1. Rating scale of Satty's analytical hierarchical process and Satty's ratio index for different numbers of variables, N.

1/9	**1/7**	**1/5**	**1/3**	**1**	**3**	**5**	**7**	**9**	
Extreme	Very strong	Strong	Moderate	Equally	Moderate	Strong	Very strong	Extreme	
	Less important			Equal		More important			
N	1	2	3	4	5	6	7	8	9
RI	0	0	0.58	0.90	1.21	1.24	1.32	1.41	1.45

Note: 1/8, 1/6, 1/4, 1/2, 2, 4, 6, 8 can also be used if a greater number of classes exist.

In this study, the definition of scores based on the relative importance of each variable was carried out by specialists in water resources, pedology, and geology, among others, associated with the physical environment, based on their expertise, specialized literature, and knowledge of the area through field campaigns carried out in 2021. In the assessment by specialists, the relative importance of the variables Land Use Adequacy and Erosion Susceptibility was similar, followed by the variables Burned Area and quantitative water balance (Table 2).

Table 2. Pairwise comparison matrix and final weight for all variables.

Criteria	**Land Use Adequacy**	**Erosion Susceptibility**	**Burned Area**	**Quantitative Water Balance**	**Weights**	**CR**
Land Use Adequacy	1.00	1.00	6.00	7.00	0.429	
Erosion Susceptibility	1.00	1.00	6.00	7.00	0.429	0.09
Burned Area	0.17	0.17	1.00	0.50	0.061	
Quantitative Water Balance	0.14	0.14	2.00	1.00	0.08	

Land Use Adequacy contains information on different levels of landscape alteration, as well as stratifying anthropogenic activities based on their impact, which is associated with the greater or lesser susceptibility of environments. Erosion Susceptibility is one of the main causes of soil degradation on the planet [28]. Furthermore, soils undergoing advanced erosive processes are areas of high environmental fragility that are difficult to restore. The variable Burned Area represents the damage caused by the direct action of fire on areas, exposing them to degradation by other agents. The variable quantitative water balance highlights the importance of water resources for the proposed environmental vulnerability index (EVI). This variable attests to the dynamics of water resources in the study area, with water availability being a decisive aspect of the capacity and speed of restoration or degradation of natural areas, as it directly affects the establishment and development of living organisms.

The AHP method evaluates the probability of uncertainty in pairwise comparisons using the principal eigenvalue and consistency index [29]. The consistency index (CI) was calculated according to Equation (1).

$$CI = \frac{\lambda_{max} - 1}{n - 1} \quad (1)$$

where λ_{max} is the significant eigenvalue of the pairwise comparison matrix and n is the number of variables.

The consistency ratio (CR) used to check the consistency of the weights indicates the probability that the values in the pair comparison matrix are randomly generated.

According to [30], a matrix with a CR greater than 0.10 should be re-evaluated. The consistency ratio was calculated using Equation (2):

$$CR = \frac{CI}{RI} \tag{2}$$

where RI is a random index. The RI values associated with different numbers of variables (N) are shown in Table 1.

A comparison matrix between the variables was developed in pairs (Table 2). Using the AHP method, the weights assigned to each thematic layer were normalized, and the values were averaged to obtain the final weights (Table 2). The calculated CR value is within acceptable limits and shows the level of consistency of the pairwise matrix.

2.4. Collection of EVI Variables

The environmental vulnerability index (EVI) results from a complex interaction between four variables, which in turn are derived from parameters directly related to environmental characteristics. These variables were selected based on the well-known relationship between them and the vulnerability of the environment, as well as the availability of data compatible with the edaphoclimatic conditions of the study area. In subsequent sections, a more detailed description of each of the four variables that make up the EVI is presented, along with the associated environmental parameters for each of these variables.

2.4.1. Land Use Adequacy

The use of land above its support capacity triggers degradation of the physical and biotic environment, which can reach levels of damage that are difficult to reverse. The suitability of land use is a very pertinent variable in indicating the environmental vulnerability of an area and is, therefore, a fundamental and selective variable for modeling the vulnerability index proposed in the present study.

The variable land use adequacy expresses the relationship between land use capability and current land use intensity in each area. The land use capability indicates the maximum potential for use of the area, considering soil characteristics, relief, and legal restrictions. This relationship directly impacts the environmental vulnerability of a given area since in places where the current land use intensity exceeds the supported use capability, there is a tendency for degradation of the physical and biotic environment with potential damage that is sometimes difficult to reverse, resulting in the unfeasibility of using the area.

The land use capability classes (LUC) follow an increasing order of limitation, ranging from I to VIII, with Class I lands those with greater resilience to more intensive uses, and Class VIII lands those with less resilience and therefore intended for less intensive uses. The determination of the land use capability class is the product, therefore, of an integrated analysis of the intrinsic characteristics of the soils, the relief [31], and the legal aspects of protection of native vegetation, as presented in Table 3.

Regarding the soil, ranking in the land use capability classes was performed from the grouping of the pedological units in the second categorical level (large groups) of the Brazilian Soil Classification System (SiBCS) [32] based on the following factors: effective depth, texture, internal drainage, flood risk, and apparent/natural fertility, as shown in Table 4. For soil classification, the pedology map of Brazil at a scale of 1:250,000 provided by the Brazilian Institute of Geography and Statistics [25] was used.

Regarding relief, the slope, which is one of the parameters that most interferes with the balance between the water that infiltrates or drains superficially into the soil, was subdivided into eight intervals of land use capability classes (Table 4), as proposed by [33]. The slope map was calculated using the Digital Elevation Model (DEM) of the study area, obtained from NASADEM images with 30 m resolution [34].

Table 3. Description of the Land Use Capability Classes (LUC).

LUC	Description
I	Land suitable for all uses, including intensive agriculture without intensive conservation practices
II	Land suitable for crops with simple conservation practices
III	Land suitable for crops with intensive or complex conservation practices
IV	Land suitable for occasional annual crops, limited perennial crops, crops in rotation with pastures, forests, and protection of wild fauna and flora
V	Land with little to no risk of erosion but with limitations impractical to be removed that greatly limit its use. Hence, it is more suitable for pasture, reforestation, or wildlife
VI	Land with severe limitations, generally unsuitable for crops, and limited use for pastures, planted forests, or native forests as a refuge for wild flora and fauna
VII	Land with very severe limitations, unsuitable for crops, limited use for pastures, planted forests, and refuge of wild flora and fauna
VIII	Land with limitations that prevent its use for any agricultural activity, restricting them to recreation and/or protection of wild flora and fauna or even water storage (dams)

Table 4. Land use capability classes (LUC) related to soil classes and slope.

Soil Class—SiBCS	Soil Class—WRB/FAO	LUC	Slope (%)	LUC
Cambissolo Húmico Cambissolo Háplico	Cambisol	VII	0–2	I
Plintossolo Pétrico Plintossolo Háplico	Plinthosols	VII V	2–5	II
Gleissolo Melânico Gleissolo Háplico	Gleysols	VIII	5–10	III
Latossolo Amarelo Latossolo Vermelho Amarelo Latossolo Vermelho	Ferralsols	II	10–20	IV
Nitossolo Vermelho	Nitisols	III	20–30	V
Argissolo Vermelho Amarelo Argissolo Vermelho	Acrisols	III	30–45	VI
Neossolo Litólico Neossolo Quartzarênico	Leptsols Arenosols	VIII V	45–70	VII
Neossolo Flúvico Luvissolo Crômico	Fluvisols Luvisols	I III	>70	VIII

Note. Adapted from [32].

As for the legal aspects, we considered the limitations of use in water permanent preservation areas (PPA) (springs and streams) and legal reserve areas (areas self-declared in the Rural Environmental Registry—CAR), imposed by the Brazilian Law of Protection of Native Vegetation (Law 12.651/2012), being assigned to these areas the land use capability Class VIII. The permanent preservation areas were obtained from the mapping performed by the Brazilian Foundation for Sustainable Development on a scale of 1:25,000 [35], and the legal reserve areas were obtained from the landowners' registrations in the CAR [36].

The land use capability class (LUC) was then defined as that corresponding to the limiting factor between the criteria related to soil, relief, and legal aspects, i.e., for a given area, the value of land use capability corresponds to the highest capability class value presented for the three criteria.

For the assessment of land use intensity, we utilized land use and land cover mapping of the study area obtained from Collection 6 of the Annual Mapping of Land Use and Land Cover in Brazil Project, MapBiomas, published in August 2021, which presents data on land use and land cover in 2020 [21]. The use and cover variable indicates how the land is being used and can be considered an indicator of current land use intensity (LUI) when the use classes are associated with different weights. Thus, the current land use intensity class was defined from the current land use and land cover (LULC) map, as classified in Table 5.

Table 5. Current land use intensity classes (LUI).

Land Use and Land Cover	LUI
Forest Formation	VIII
Savanna Formation	VI
Silviculture	VI
Other Non-Forest Formations	VIII
Flooded Field and Swampy Area	VIII
Grasslands	VIII
Pastures	III
Agriculture	II
Mosaic of Uses	II
Urbanized Area	I
Other Non-Vegetated Areas	I
Mining	I
Rocky Outcrop	VIII
Water Body	VIII

Based on the land use capability class (LUC) and land use intensity (LUI) obtained previously, the number of exceeding classes (NCE) was determined, which represents how much land is being used in relation to its capacity (Equation (3)).

$$NCE = LUC - LUI \quad (3)$$

where NCE = number of exceeding classes, LUC = land use capability class, dimensionless, and LUI = land use intensity, dimensionless.

As there are eight land use capability classes in the classification system used, the equation allows for results ranging from 7 to −7, with positive, negative, and null results indicating, respectively, that the soil is being used above, below, and in accordance with its use capability. The negative values were converted to null, as they are not considered vulnerable areas since they are being used below their capacity, and the values of the adequacy classes from 0 to 7 were converted to a scale from 0 to 1 to standardize with the other maps used in the AHP multicriteria analysis.

2.4.2. Burned Area

Fire can be extremely damaging to the environment, as areas with fire occurrence have their biota severely affected and, in addition, become exposed and susceptible to physical, chemical, and biological degradation processes. This damage is intensified in sensitive ecosystems, such as the Atlantic Rainforest and Cerrado environments. This is because, historically, Atlantic Forest species have not been subjected to recurrent fires that require physiological and structural adaptations for survival. In contrast, the Cerrado has evolved with fire as a natural component of its ecosystem, leading to different adaptive strategies among its species [37].

Despite being a natural component of the Cerrado, the intense process of human intervention in the environment has altered the origins of fires and subjected ecosystems to frequencies and intensities of disturbances to which species are probably not adapted [38]. Therefore, fire is a significant source of environmental degradation in river basins with an advanced process of anthropization, as is the case in the SFRB. Thus, studying and evaluating the occurrence of fires in this basin is fundamental for mitigating their impacts on fauna, flora, and soil properties.

The burned areas were evaluated using the fire scar maps of Brazil for the period of 2011 to 2020, developed by MapBiomas, from Landsat satellite images with 30 m spatial resolution, available on the project's website [39]. The map of fire scars for each year was summed to assess the recurrence of fires in the ten-year period (2011 to 2020). Thus, the areas that did not burn at all during the analyzed period received a value of zero, and the remaining areas that burned at least once received values between 1 and 10, depending on the number of years in which the fires recurred in the period. Subsequently, the recurrence values of the burned areas were converted to a scale of 0 to 1 to standardize the other maps used in the AHP multicriteria analysis.

2.4.3. Erosion Susceptibility

Water erosion is one of the main forms of soil degradation and is responsible for over 70% of the degraded areas worldwide. Thus, natural erosion potential is characterized as a relevant indicator of environmental vulnerability, which is why this variable was used as a criterion for obtaining the proposed environmental vulnerability index (EVI) in the present study.

Human activity and changes related to land use are the main causes of accelerated soil erosion, which has substantial implications for the nutrient and carbon cycle, the productive capacity of the land, and, consequently, the socioeconomic conditions of river basins [40]. Therefore, to mitigate erosion processes, it is necessary to know about soil types, topography, natural or artificial drainage, and slope stability conditions in order to adapt the soil cover to each specific situation.

In this context, one of the ways to provide subsidies for the selection of priority areas for the conservation and recovery of native vegetation is the use of spatialized maps of natural soil erosion potential. In this study, a methodology was proposed for obtaining the erosion susceptibility map for the headwaters of the SFRB by means of the weighted average of the rainfall erosivity (R), soil erodibility (K), and slope (S), scaled from 0 to 1. According to the characteristics of the study area, the expertise of the authors, and simulations carried out with different combinations of weights, the weights shown in Equation (4) were considered, where soil erodibility was twice as important as the other parameters considered when calculating erosion susceptibility (ES).

$$\text{ES} = (0.5 \times \text{K}) + (0.25 \times \text{R}) + (0.25 \times \text{S}) \quad (4)$$

where ES = erosion susceptibility, R = rainfall erosivity factor map, K = soil erodibility factor map, and S = slope map, all of which were rescaled to a scale of 0 to 1.

Rainfall Erosivity (R)

Rainfall erosivity expresses the capacity of rainfall expected in each location to cause erosion of bare soil [41]. It is related to the impact of the drops, which, due to their kinetic energy, break down the soil aggregates, making them lighter and more susceptible to being washed away by surface runoff. The rainfall erosivity map was obtained by adding up the monthly values of the erosion indices (R), which were calculated using Equation (5) proposed by [42].

$$\text{R} = 20,411\left(\frac{\text{p}^2}{\text{P}}\right) + 181.45 \quad (5)$$

where p = average monthly rainfall and P = average annual rainfall.

The rainfall data needed to apply this equation were obtained from TerraClimate for the period from 2001 to 2020 [12]. The erosivity map was then rescaled from 0 to 1 to standardize the scale with other erosion susceptibility maps.

Soil Erodibility (K)

Soil erodibility represents the susceptibility of a given type of soil to erosive processes, i.e., the ease with which soil particles are detached and transported by the impact of raindrops and surface runoff [43,44]. This characteristic is related to the soil's physical properties, such as texture, structure, density, and permeability, as well as the soil's chemical, biological, and mineralogical properties [45].

The soil erodibility map was obtained by analyzing the existing soil classes weighted by the lithological units of the geology maps [25], with susceptibility values ranging from 1 to 5, as shown in Table 3. These values were assigned based on the criteria for assessing the erosion potential of different Brazilian soils proposed by [46,47]. The final weight of soil erodibility was calculated using the weighted average between the weights of the soil class and geological component, according to Equation (6).

$$K = 0.6 \times WKS + 0.4 \times WKG \quad (6)$$

where K = soil erodibility factor, WKS = weight of the soil component in the soil erodibility factor, and WKG = weight of the geological component in the soil erodibility factor.

Slope (S)

Relief is another aspect of fundamental importance for understanding and quantifying the erosion process, with slope and slope length being the main relief variables related to erosion. The greater the slope, under the same soil and rainfall conditions, the smaller the volume of water that effectively infiltrates the soil, and consequently, the greater the volume and energy associated with runoff [48]. The influence of relief on susceptibility to erosion can be represented by the slope of the land.

In this work, the slope map was calculated using the Digital Elevation Model (DEM) of the study areas, obtained from NASADEM images with a resolution of 30 m [23]. This map was then rescaled from 0 to 1 to standardize the scale with other erosion susceptibility maps.

2.4.4. Quantitative Water Balance

Quantitative water balance is of fundamental importance for the diagnosis of the level of water commitment in river basins, which is being carried out in Brazil by river reach and micro basin by the National Water and Basic Sanitation Agency (ANA). Its role is to identify how much of the available water is being used to satisfy consumptive uses. This is given by the ratio between demand and supply and is presented in terms of the percentage of impairment.

Demand corresponds to the sum of the estimated withdrawal flows for the various sectoral consumptive uses associated with their place of use, without distinction between surface and underground uses. An exception applies to the urban supply, whose flow is associated with the withdrawal point, and only the surface portion is accounted for. The supply, in turn, corresponds to a high guaranteed flow rate, defined as water availability, and aggregates the Q_{95} flow rate (flow rate with permanence at 95% of the time) and the additional flow offered by reservoirs according to their operating mode [49].

The current data distributed in micro basins were constructed in a scenario of current water balance, with demands for 2020. In this scenario, the water balance was carried out by river reach, classifying the level of water commitment of the reaches as low (below 5%), medium (5% to 30%), high (30% to 70%), very high (70% to 100%), critical (above 100%), and intermittent (zero supply) [49].

For use in the AHP multicriteria analysis, the quantitative water balance values were converted to a scale of 0 to 1 to standardize with maps of the other variables, where the value 1 was assigned to critical micro basins and zero to those with low commitment.

3. Results and Discussion

3.1. Environmental Vulnerability Index (EVI)

3.1.1. Land Use Suitability

Land use capability was defined as the variable corresponding to the limiting factor between the criteria related to soil, relief, and legal aspects; that is, for a given area, the value of land use capability corresponds to the highest value of the capability class presented for the three criteria. Figure 3a presents the land use capability map of the studied basin, in which it is possible to observe that land use capability classes II, III, VII, and VIII are those that predominate in the basin, corresponding together to about 90.2% of its total area.

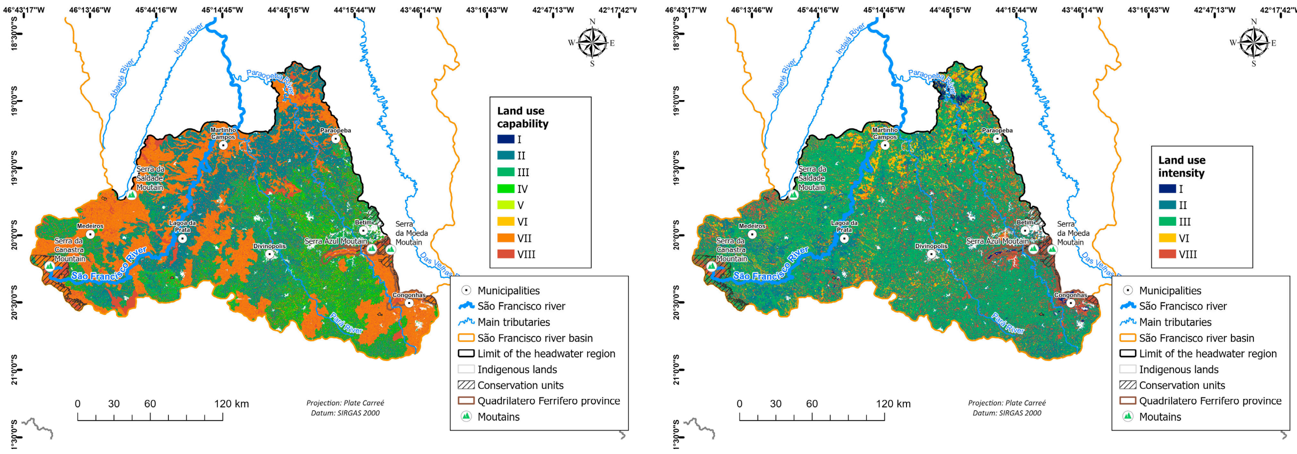

(**a**) (**b**)

Figure 3. (**a**) Land use capability and (**b**) land use intensity in the headwaters of São Francisco.

A large part of the headwaters of the SFRB, 49.8% of the total area, fell into classes VII and VIII, i.e., lands with very severe limitations, unsuitable for crops and of restricted use for pastures, planted forests, and refuge for wild flora and fauna, or even with limitations that prevent their use for any agricultural activity, restricting them to recreation and/or protection of wild flora and fauna, or even water storage. It is also observed that 20.1% of the areas were classified as Class II, which are lands suitable for crops with simple conservation practices, while 20.3% were classified as Class III, which are lands suitable for crops with intensive or complex conservation practices. The remaining areas, about 9.8% of the basin, were classified as classes I, IV, V, and VI.

The classification of the current land use map of the study area generated a land use intensity map (Figure 3b). According to the proposed classification, about 26.6% of the basin area is currently with the intensity of use in classes I and II, which are considered the most intense use classes related to agriculture, mining, and non-vegetated areas. About 45% of the basin is in Class III, related to the presence of pastures, while 28.4% is in classes VI and VIII, which are considered less intense when compared to the other classes and are associated with natural formations and silviculture.

The number of exceeding classes was calculated by subtracting the land use intensity (LUI) from the land use capability class (LUC), representing how much land is being used beyond its capacity. Figure 4 presents a map of exceeding land use capability classes in the headwaters of the SFRB, in which it is possible to observe that approximately 49.4% of the studied basin area presents land use intensity below or equal to the use capability, while 50.6% of the basin area presents use intensity above the capability, with 33.5% of the areas exceeding four to six classes of use intensity.

The areas with the highest number of exceeding classes are located mostly in the western region of the basin and are associated mainly with areas with highly erodible soils, such as Leptsols and Cambisol with high slopes, being used for uses such as pastures and agriculture. The combination of these three parameters represents the most intensive scenario in the region, exerting the greatest pressure and resulting in the worst situation in terms of land use. We also observed areas with a high number of exceeding classes in areas protected by legal aspects, such as legal reserve areas (LR) and permanent preservation areas (PPA), which have current use diverging from that defined by law. For the application of the AHP multicriteria analysis, this map was later converted into a common scale from 0 to 1 in order to standardize with the other maps.

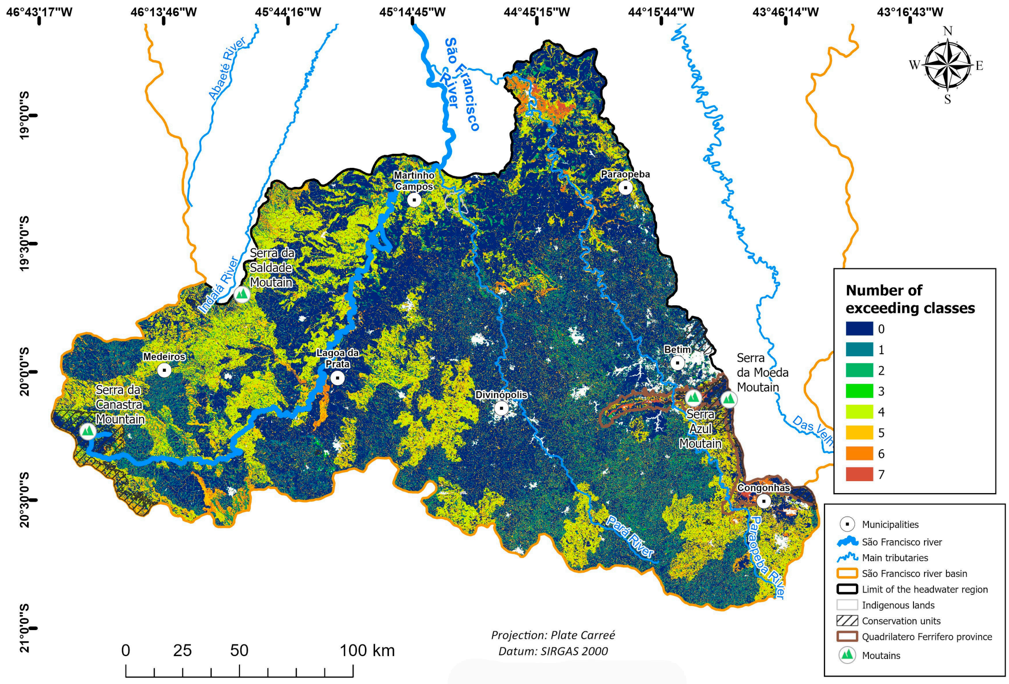

Figure 4. Number of exceeding classes in the headwaters of the São Francisco River Basin.

3.1.2. Burned Area

The recurrence map of burned areas in the headwaters of the SFRB (Figure 5) shows that 95.98% of the area of the headwaters has not been burned in the last ten years, and only 4.0% of the area has been burned during this period. In 1.0% of the area, there was a recurrence of fires, i.e., places where fires were detected in two or more years within the period analyzed. The detection of fires in the same region occurred in up to seven of the ten years analyzed. In general, however, the environmental vulnerability of the headwaters of the SFRB was low in terms of burned areas during the period analyzed.

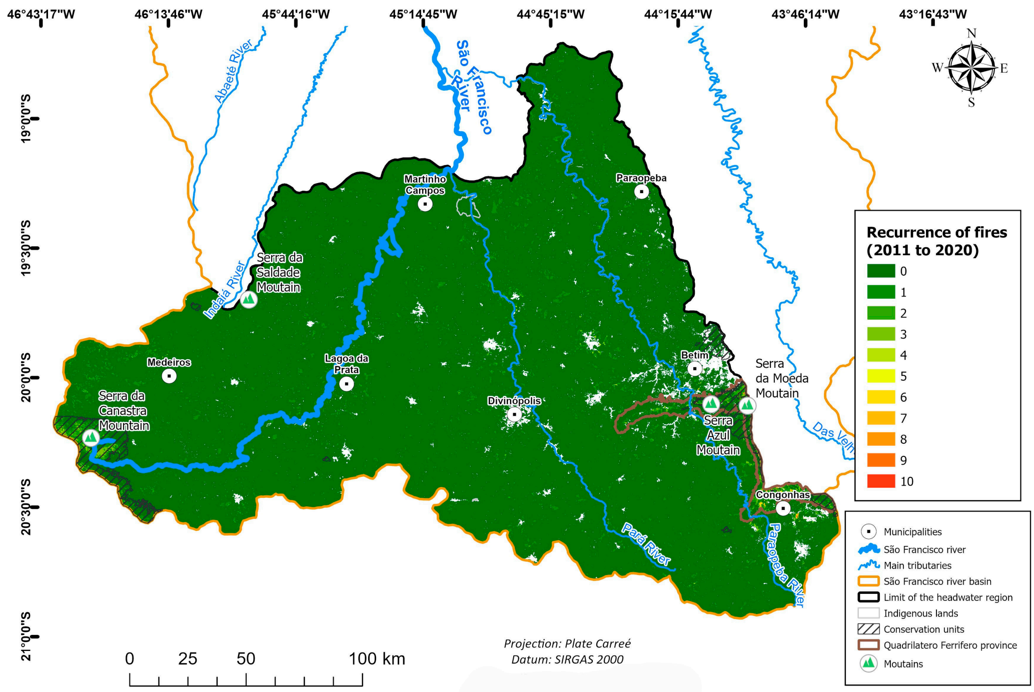

Figure 5. Recurrence of fires in the headwaters of the São Francisco River Basin.

It can be seen that the highest frequency of fires is found in areas in the far west of the basin, in the Serra da Canastra National Park, where the vegetation formed by the grassy stratum of grassland formations tends to dry out during periods of drought and favors the spread of fires in the region. Other areas of fires coincide with the route of roads and proximity to large urban centers in the Paraopeba Basin, corroborating other studies that show high incidences of fire ignition caused by human actions around accessibility networks [50–52].

3.1.3. Erosion Susceptibility

Rainfall erosivity in the headwaters of the SFRB varied between 5646 and 7006 MJ mm^{-1} ha^{-1} h^{-1} year^{-1} and its pattern is mainly associated with the distribution of rainfall in the basin (Figure 6a), with the highest rainfall erosivity values, above 6500 MJ mm^{-1} ha^{-1} h^{-1} year^{-1}, being found in the southeast of the basin, mainly in the highest and steepest parts, related to the western edge of the province known as Quadrilatero Ferrifero, one of the richest mineral-bearing regions in the country, more specifically along the Azul and Moeda mountain ranges.

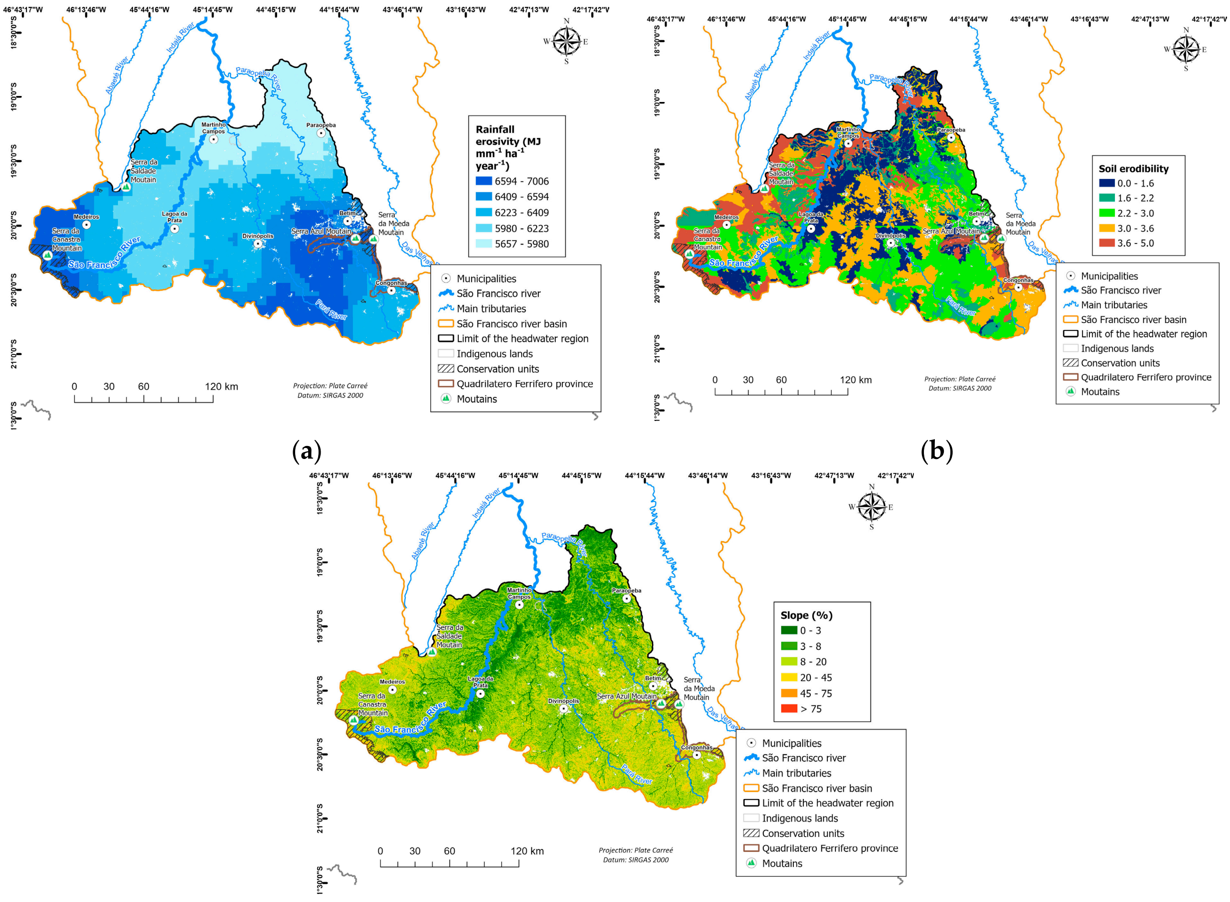

(**a**) (**b**) (**c**)

Figure 6. (**a**) Rainfall erosivity, (**b**) soil erodibility, and (**c**) slope of the headwaters of the São Francisco River Basin.

Figure 6b shows the map of soil erodibility in the headwaters of the SFRB. The areas with the highest soil erodibility are located mainly in the eastern and central regions of the headwaters and are mainly related to the presence of Cambisols in Neoproterozoic pelitic rocks belonging to the Bambuí Group. These sedimentary rocks, which are often stratified parallel to the surface, show a certain resistance to weathering and thus lead to the occurrence of poorly developed soils, such as Cambisols and, to a lesser extent, Leptsols. These soils are often covered by gravelly surfaces and develop pronounced surface sealing.

The combination of these two characteristics makes them highly susceptible to erosion, as they hinder water infiltration and, consequently, the growth of larger vegetation. In these areas, the predominance of surface runoff over infiltration, combined with the predominant use of extensive pastures, leads to intense erosion processes.

On the western edge of the headwaters, there is also an extensive area with high erosion susceptibility. As in the central region, these are pelitic and metapelitic rocks (siltstones, shales, and slates), also belonging to the Bambuí Group. However, on the western edge, the stratigraphy of these rocks is practically perpendicular to the surface, representing a border region folded by post-Proterozoic metamorphic processes. This is because it is the contact zone between these sedimentary layers, which lie on the crystalline rocks of the São Francisco craton and the metamorphic rocks of the southern portion of the Brasília-Tocantins Mobile Belt. This contact is expressed by a gap, locally known as the Saudade Mountain, which separates two dissected plateaus. In these areas, erosion processes are very intense, and high slope gradients are added to the soil's intrinsic characteristics.

Another important area with high susceptibility to erosion is in the extreme southeast of the basin and is represented by the western flank of the Quadrilátero Ferrífero geological province. This is an intensely folded area, consequently with a very steep terrain, where shallow and poorly developed soils predominate, such as Cambisols and Leptsols sitting on metamorphic rocks, such as phyllites, schists, itabirites, quartzites, and others.

The main relief classes found in the headwaters of the SFRB are wavy (43.8%), gently wavy (26.7%), and strongly wavy (16.9%) (Figure 6c). The mountainous and steep terrain occupies only 1.1% of the area of the headwaters, and the plain terrain is present in 11.5% of the total area. The flat part of the basin's headwaters is mainly located on a strip close to the right bank of the São Francisco River. This relief, which is predominantly smoothed, reduces the susceptibility to erosion processes, even with the predominance of pastures as the main land cover. Areas with a slope of over 45% are associated with mountain regions, such as the Moeda, Azul, Canastra, and Saudade mountains.

The susceptibility to erosion in the SFRB (Figure 7) was obtained through the product of the rainfall erosivity, soil erodibility, and slope, using Equation (4). The areas with the greatest susceptibility to erosion are those located in the western and southeastern parts of the basin, where there are the highest rainfall rates, and the pedological units with the greatest susceptibility to erosion, such as Cambisols and Leptsols. In the southeast of the basin, there are areas of greater slope associated with Paleoproterozoic geological formations linked to the Quadrilatero Ferrifero province. In the extreme southwest, the presence of areas of high slope is linked to rocks of the Araxá Group of the Neoproterozoic age. Along the western edge and in the center of the basin, the areas of a greater slope, and consequently, more susceptible to erosion, are linked to the presence of pelitic and metapelitic rocks of the Bambuí Group, also of Neoproterozoic age, on which shallow soils develop, where the processes of surface runoff take precedence over infiltration and pedogenesis.

3.1.4. Quantitative Water Balance

The quantitative water balance in the headwaters of the SFRB (Figure 8) shows that around 93.7% of the basin area has excellent or comfortable water availability. In the remaining 6.3% of the area, availability was classified as worrying, critical, or very critical. For the headwaters of the SFRB, the sub-basins with very critical water availability are mainly located near urban centers, where the demands for human supply and industrial uses are higher.

3.1.5. EVI

After standardizing the environmental variables on a scale of 0 to 1, they were multiplied using map algebra, applying the weights in Table 2, and generating the final map of the environmental vulnerability index (EVI) in the headwaters of the SFRB (Figure 9). The EVI map was subdivided into five classes of equal areas: very low, low, medium, high, and very high. Values close to 1 correspond to areas with very high EVI, while values close to 0 are associated with regions characterized by very low EVI. The areas with the highest EVI values are mainly related to areas with shallow and easily erodible soils, such as Leptsols and Cambisols, associated with areas with high slopes, being used predominantly for pasture and, to a lesser extent, for agricultural plantations. This combination of parameters, as previously mentioned, accentuates environmental vulnerability. It represents the most intensive scenario with the greatest environmental pressure.

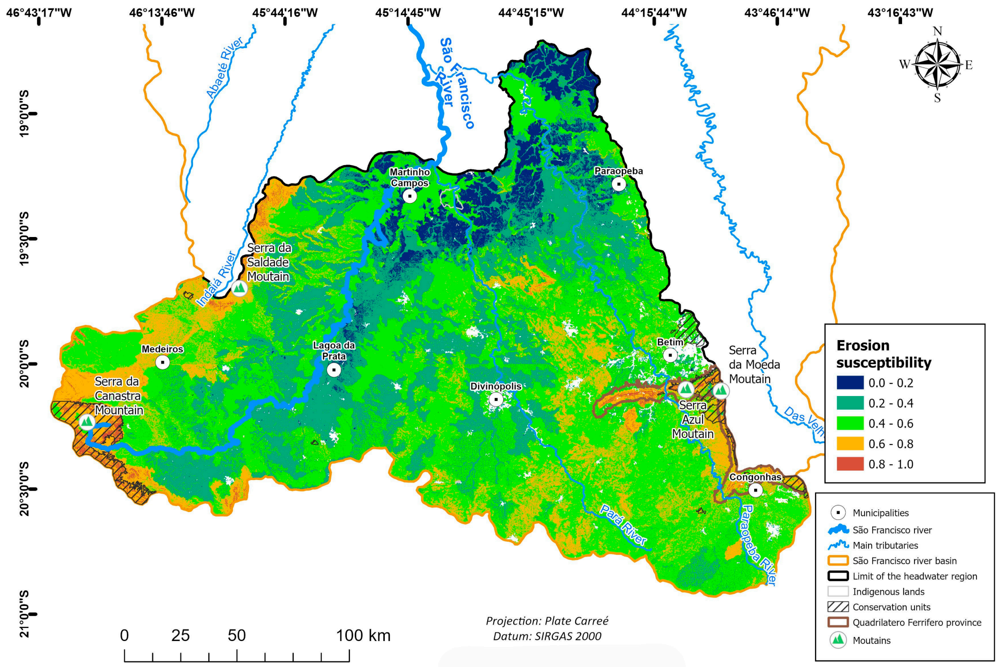

Figure 7. Erosion susceptibility in the headwaters of the São Francisco River Basin.

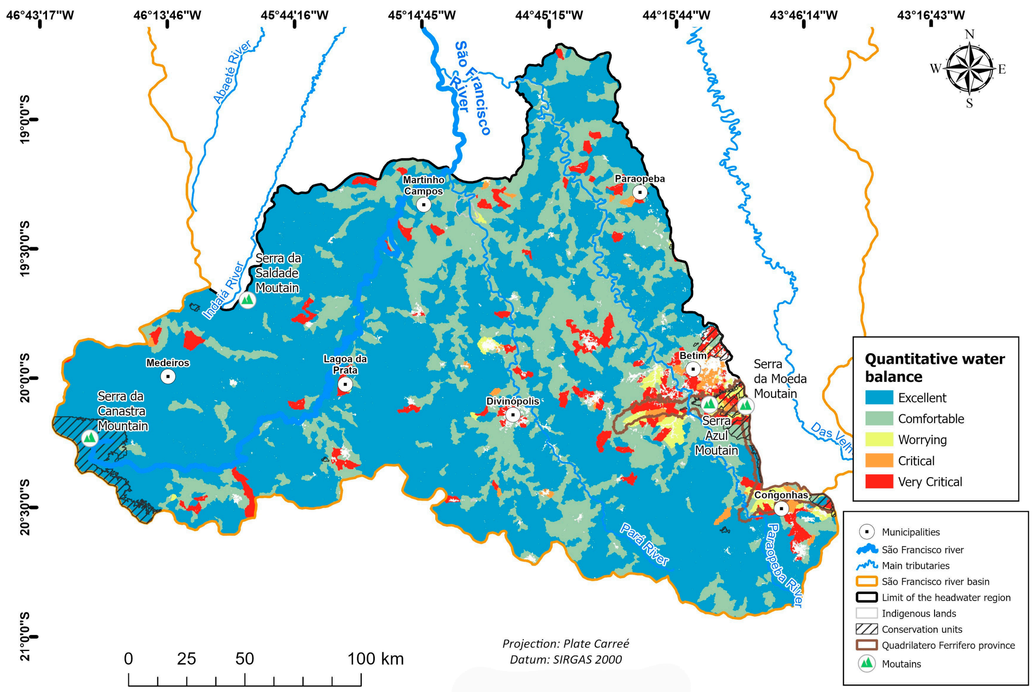

Figure 8. Quantitative water balance in the headwaters of the São Francisco River Basin.

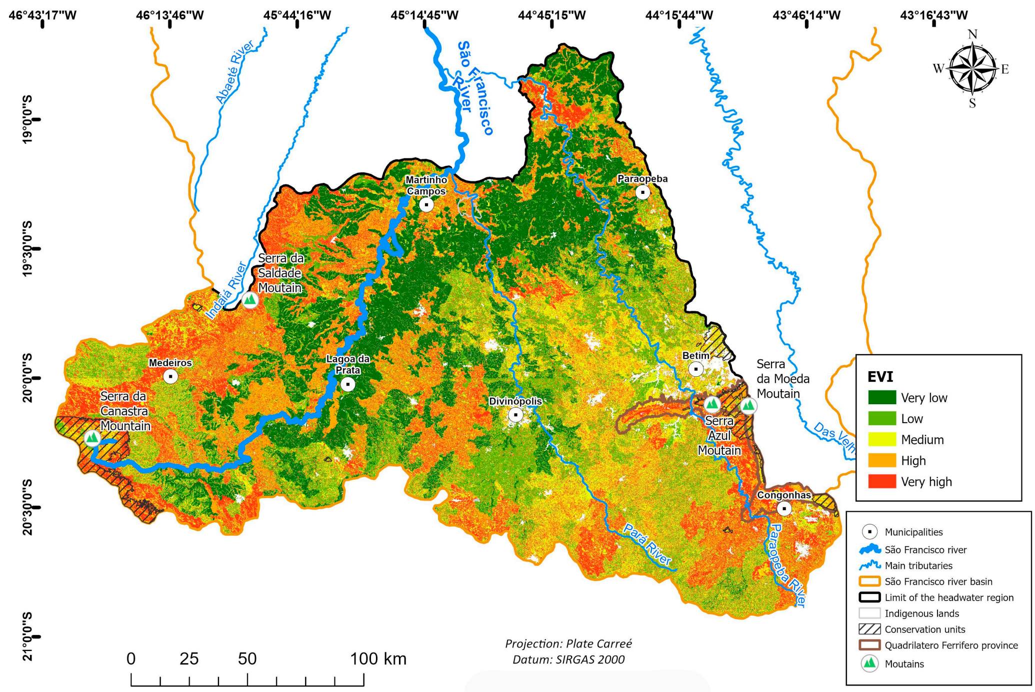

Figure 9. Environmental Vulnerability Index (EVI) in the headwaters of the São Francisco River Basin.

Since the Brazilian colonial period, the SFRB has been used for extensive cattle raising, mining, and the implementation of large steel industrial actions, promoting the clearing of native vegetation from land for charcoal production. More recently, increases in agricultural production, mainly soybean, corn, and sugarcane, have been observed, leading to intensified land clearing and associated to increased soil erosion rates. According to [53], in 2022, the deforested area in the headwaters of the SFRB was 3444.5 ha, of which 2660.3 ha (77.2%) were in the Cerrado, while 784.2 ha (22.8%) were in the Atlantic Forest.

The EVI values were also high in the areas with the highest number of exceeding classes, in areas protected by legal aspects, such as Water PPAs and Legal Reserves, which currently have more intensive uses than defined by law, such as pasture, exposed soil, and crops. Areas close to conservation units and indigenous lands also showed high EVI values, indicating human pressure in fully protected areas (Figure 9). A similar result was found by [9], who analyzed the environmental vulnerability of the SFRB to drought conditions and land degradation. They found that for the entire SFRB, the highest vulnerability values occurred within a 5 km buffer in relation to the conservation units, representing approximately 32.4% of the total area.

Also noticeable in areas with high EVI values is the influence of the critical and very critical sub-basins in relation to water availability, located in the north-central and extreme eastern regions of the basin, the latter being related to the large urban centers of the Belo Horizonte metropolitan region. The municipality of Belo Horizonte alone serves 2,402,829 inhabitants with treated water, with an average consumption of 156.5 L/person/day [54], which has a direct impact on the water availability of the tributaries of the São Francisco River, especially of the Paraopeba River.

The Burned Area variable received a lower weight than the other variables (6.1%), which reflects its lower influence on the final EVI map. However, areas with higher fire frequency, mainly in the western region of the basin near Serra da Canastra and in the eastern region near the Quadrilatero Ferrifero province, coincide with high EVI areas. In these regions, altitudes are mostly above 1000 m, with the presence of natural vegetation, such as high-altitude grasslands and rocky fields dominated by shrubs and grasses.

Regular fires are a part of these ecosystems due to the microclimatic conditions associated with altitude and the type of vegetation present, as well as the proximity of human activities that make these environments prone to fires. The predominant vegetation, com-posed of grasses and shrubs, provides highly flammable fuel, facilitating the spread of fire. Additionally, climatic conditions such as high temperature, low humidity, and frequent winds create a favorable environment for fire ignition and propagation [33].

It can also be seen in Figure 9 that the areas with the highest environmental vulnerability indices are in the west and southeast of the headwaters of the SFRB, in the São Francisco 01 and Paraopeba sub-basins, respectively. This result makes it possible to select priority areas for intervention, where the implementation of recovery or mitigation actions will enable the greatest preservation and, consequently, the greatest potential return of desirable ecosystem services. In countries like Brazil, where the scarcity of resources limits environmental preservation actions, it is extremely important to identify the areas where recovery measures are most needed to effectively allocate the available funds.

The EVI exhibits a notable advantage over other environmental indices: the robustness of its constituent variables. When compared to similar indices, such as those developed by [55,56], it is evident that the EVI incorporates all the variables employed in these studies. Ref. [55] focused on the Caratinga River watershed, while [56] analyzed water supply systems in a major southeastern metropolis. Despite their differing scopes, both studies utilized variables that were comprehensively represented within the EVI.

Two primary variables commonly utilized in environmental vulnerability assessments, land use and land cover, as well as land use capacity, are prominently represented in the literature [55–60]. This underscores the crucial role that these variables play in such analyses. The EVI's distinctive approach involves a preliminary examination of the interplay between land use and land cover, a metric termed 'Land Use Intensity'. This procedure facilitates precise identification of the correlation between land use capacity and intensity, thereby supporting the robustness of the 'Land Use Adequacy' variable.

On the other hand, a notable limitation of the EVI is its current lack of comprehensive socioeconomic variable integration. Given their crucial role in understanding the anthropogenic influence on the environment, incorporating these variables could significantly enhance the EVI's analytical capabilities. Numerous studies, especially those conducted at broader geographic scales, have demonstrated the efficacy of integrating socioeconomic factors into environmental vulnerability assessments, as exemplified by research [58,59].

4. Conclusions

In recent decades, several socio-environmental indices have been proposed in Brazil, most of which are related to natural threats, such as disasters related to flood risk in metropolitan areas [61,62], or to anthropogenic threats, such as disasters related to mining dam ruptures [63]. However, few indices have proposed a global application with the aim of indicating areas for environmental recovery, and none of these have been applied to the São Francisco River Basin (SFRB).

In this paper, we present a new approach to characterizing and quantifying environmental vulnerability, integrating geospatialized indicators of specific importance to the study area, considering relief, hydrology, pedology, geology, climate, and land use aspects. Four variables were selected as the main criteria for defining the environmental vulnerability index (EVI): Land Use Adequacy, Burned Area, Erosion Susceptibility and quantitative water balance. We present a well-established approach in the literature for defining the environmental vulnerability index, applying the AHP multicriteria analysis associated with the expertise of Brazilian specialists in the areas of pedology, geology, hydrology, and natural sciences to understand the spatial variability of environmental vulnerability in the area of study. Although the consistency ratio of the AHP multicriteria analysis highlights the robustness of the methodology presented here, other approaches that minimize some level of subjectivity that exists in the experts' analysis are desirable developments for future research. The EVI was applied to the headwaters of the SFRB, and we observed that, according to the AHP analysis, the factors Land Use Adequacy and Erosion Susceptibility had the greatest influence on environmental vulnerability in the headwaters of the SFRB, together explaining 83.6% of the EVI, while the factors quantitative water balance and Burned Areas had less influence on the final index.

The areas with the highest EVI are mainly related to the presence of shallow and easily erodible soils, such as Leptsols and Cambisols, associated with areas with steep slopes and used predominantly as pastures and agricultural crops. This combination of parameters represents the most intensive scenario with the greatest environmental pressure. In addition, high EVI values are found in the areas with the highest number of exceeding classes of land use, which are also related to very critical and critical basins in terms of water availability, located close to urban centers. A limitation of this study can be highlighted by the fact that ecological threats linked to seasonal climate variations, which can generate extreme drought or flood events, are not necessarily addressed in areas with high EVI values.

A major contribution of this study is the identification of an environmental vulnerability index, considering the regional climate, fire, soil susceptibility to erosion, land use dynamics, and legal aspects. The EVI presents itself as applied information and is useful as a tool in directing government and private environmental recovery programs geographically targeted to regions of greater vulnerability. This allows managers and territorial agents to direct resources and act more incisively in priority areas. The results of this work can directly point out areas where reforestation work should be prioritized or where soil and water conservation practices need to be applied in agricultural management, thus increasing the provision of ecosystem services based on a balance between the use and conservation of natural resources.

Author Contributions: Conceptualization, C.D.C., D.D.d.S. and R.S.S.A.; methodology, C.D.C., B.N.F.V., E.L.P., E.I.F.F. and P.C.B.; software, C.D.C. and L.V.S.; validation, D.D.d.S., R.S.S.A. and E.I.F.F.; formal analysis, C.D.C. and E.L.P.; investigation, C.D.C., E.L.P. and P.C.B.; resources, J.A.F.N.; data curation, C.D.C., E.L.P., R.S.S.A., P.C.B. and E.I.F.F.; writing—original draft preparation, C.D.C.; writing—review and editing, C.D.C., R.S.S.A., E.L.P. and B.N.F.V.; visualization, C.D.C.; supervision, D.D.d.S. and J.A.F.N.; project administration, J.A.F.N.; funding acquisition, D.D.d.S. and J.A.F.N. All authors have read and agreed to the published version of the manuscript.

Funding: This research was funded by Ministério da Integração e do Desenvolvimento Regional (MDR) and Conselho Nacional de Desenvolvimento Científico e Tecnológico (CNPq), grant number 150171/2022-6.

Data Availability Statement: The raw data supporting the conclusions of this article will be made available by the authors upon request.

Acknowledgments: The authors would like to express their gratitude to Conselho Nacional de Desenvolvimento Científico e Tecnológico (CNPq), Coordenação de Aperfeiçoamento de Pessoal de Nível Superior (CAPES), and Ministério da Integração e do Desenvolvimento Regional (MDR), for their financial support for the project under which this research was carried out.

Conflicts of Interest: The authors declare no conflicts of interest.

References

1. Pompeu, J.; Assis, T.O.; Ometto, J.P. Landscape Changes in the Cerrado: Challenges of Land Clearing, Fragmentation and Land Tenure for Biological Conservation. *Sci. Total Environ.* **2024**, *906*, 167581. [CrossRef] [PubMed]
2. Barnett, J.; Lambert, S.; Fry, I. The Hazards of Indicators: Insights from the Environmental Vulnerability Index. *Ann. Assoc. Am. Geogr.* **2008**, *98*, 102–119. [CrossRef]
3. Akintan, O.B.; Olusola, J.A.; Imole, O.P.; Adeyemi, M.O. Geotechnical and GIS-Based Environmental Factors and Vulnerability Studies of the Okemesi Landslide, Nigeria. *Reg. Sustain.* **2023**, *4*, 249–260. [CrossRef]
4. Peruchi Trevisan, D.; da Conceição Bispo, P.; Almeida, D.; Imani, M.; Balzter, H.; Eduardo Moschini, L. Environmental Vulnerability Index: An Evaluation of the Water and the Vegetation Quality in a Brazilian Savanna and Seasonal Forest Biome. *Ecol. Indic.* **2020**, *112*, 106163. [CrossRef]
5. Padilha, D.G.; Luiz Trevisan, M.; Cabral Cruz, J. Sensibilidade Do Modelo de Fragilidades Ambientais à Ponderação Multicriterial: Aspectos Físicos Da Bacia Hidrográfica Do Alto Uruguai. *Floresta* **2014**, *44*, 535–548. [CrossRef]
6. Zou, T.; Yoshino, K. Environmental Vulnerability Evaluation Using a Spatial Principal Components Approach in the Daxing'anling Region, China. *Ecol. Indic.* **2017**, *78*, 405–415. [CrossRef]

7. Li, L.; Shi, Z.H.; Yin, W.; Zhu, D.; Ng, S.L.; Cai, C.F.; Lei, A.L. A Fuzzy Analytic Hierarchy Process (FAHP) Approach to Eco-Environmental Vulnerability Assessment for the Danjiangkou Reservoir Area, China. *Ecol. Modell.* **2009**, *220*, 3439–3447. [CrossRef]
8. Li, A.; Wang, A.; Liang, S.; Zhou, W. Eco-Environmental Vulnerability Evaluation in Mountainous Region Using Remote Sensing and GIS—A Case Study in the Upper Reaches of Minjiang River, China. *Ecol. Modell.* **2006**, *192*, 175–187. [CrossRef]
9. da Silva Pinto Vieira, R.M.; Tomasella, J.; Cunha, A.P.M.D.A.; Barbosa, A.A.; Pompeu, J.; Ferreira, Y.; Santos, F.C.; Alves, L.M.; Ometto, J. Socio-Environmental Vulnerability to Drought Conditions and Land Degradation: An Assessment in Two Northeastern Brazilian River Basins. *Sustainability* **2023**, *15*, 8029. [CrossRef]
10. Luo, D.; Caldas, M.M.; Goodin, D.G. Estimating Environmental Vulnerability in the Cerrado with Machine Learning and Twitter Data. *J. Environ. Manag.* **2021**, *289*, 112502. [CrossRef]
11. Zhao, J.; Ji, G.; Tian, Y.; Chen, Y.; Wang, Z. Environmental Vulnerability Assessment for Mainland China Based on Entropy Method. *Ecol. Indic.* **2018**, *91*, 410–422. [CrossRef]
12. Marengo, J.A.; Galdos, M.V.; Challinor, A.; Cunha, A.P.; Marin, F.R.; Vianna, M.D.S.; Alvala, R.C.S.; Alves, L.M.; Moraes, O.L.; Bender, F. Drought in Northeast Brazil: A Review of Agricultural and Policy Adaptation Options for Food Security. *Clim. Resil. Sustain.* **2022**, *1*, e17. [CrossRef]
13. Wang, S.Y.; Liu, J.S.; Yang, C.J. Eco-Environmental Vulnerability Evaluation in the Yellow River Basin. *Pedosphere* **2008**, *18*, 171–182. [CrossRef]
14. Houghton, J.T.; Ding, Y.; Griggs, D.J.; Noguer, M.; van der Linden, P.J.; Dai, X.; Maskell, K.; Johnson, C.A. *IPCC Climate Change 2001: The Scientific Basis*; Cambridge University Press: Cambridge, UK, 2011.
15. Vancine, M.H.; Muylaert, R.L.; Niebuhr, B.B.; de Faria Oshima, J.E.; Tonetti, V.; Bernardo, R.; De Angelo, C.; Rosa, M.R.; Grohmann, C.H.; Ribeiro, M.C. The Atlantic Forest of South America: Spatiotemporal Dynamics of the Vegetation and Implications for Conservation. *Biol. Conserv.* **2024**, *291*, 110499. [CrossRef]
16. Myers, N.; Mittermeier, R.A.; Mittermeier, C.G.; da Fonseca, G.A.; Kent, J. Biodiversity Hotspots for Conservation Priorities. *Nature* **2000**, *403*, 853–858. [CrossRef]
17. Pires, M.O. 'Cerrado', Old and New Agricultural Frontiers. *Braz. Political Sci. Rev.* **2020**, *14*, 24. [CrossRef]
18. Jong, P.; Barreto, T.B.; Tanajura, C.A.S.; Oliveira-Esquerre, K.P.; Kiperstok, A.; Andrade Torres, E. The Impact of Regional Climate Change on Hydroelectric Resources in South America. *Renew. Energy* **2021**, *173*, 76–91. [CrossRef]
19. Freitas, A.A.; Drumond, A.; Carvalho, V.S.B.; Reboita, M.S.; Silva, B.C.; Uvo, C.B. Drought Assessment in São Francisco River Basin, Brazil: Characterization through SPI and Associated Anomalous Climate Patterns. *Atmosphere* **2022**, *13*, 41. [CrossRef]
20. CBHSF. The River Basin. Available online: https://cbhsaofrancisco.org.br/a-bacia/ (accessed on 30 July 2024).
21. MapBiomas Coleção 6 Da Série Anual de Mapas Da Cobertura e Uso Do Solo Do Brasil. Available online: https://mapbiomas.org/ (accessed on 4 October 2022).
22. Beck, H.E.; McVicar, T.R.; Vergopolan, N.; Berg, A.; Lutsko, N.J.; Dufour, A.; Zeng, Z.; Jiang, X.; van Dijk, A.I.J.M.; Miralles, D.G. High-Resolution (1 Km) Köppen-Geiger Maps for 1901–2099 Based on Constrained CMIP6 Projections. *Sci. Data* **2023**, *10*, 724. [CrossRef]
23. Abatzoglou, J.T.; Dobrowski, S.Z.; Parks, S.A.; Hegewisch, K.C. TerraClimate, a High-Resolution Global Dataset of Monthly Climate and Climatic Water Balance from 1958–2015. *Sci. Data* **2018**, *5*, 170191. [CrossRef]
24. Copernicus Climate Change Service. (C3S): ERA5: Fifth generation of ECMWF Atmospheric Reanalyses of the Global Climate. Copernicus Climate Change Service Climate Data Store (CDS) 2017. Available online: https://cds.climate.copernicus.eu/cdsapp#!/home (accessed on 23 August 2024).
25. IBGE Pedologia 1:250,000. Available online: https://www.ibge.gov.br/geociencias/informacoes-ambientais/pedologia/10871-pedologia.html?=&t=downloads (accessed on 26 November 2023).
26. Saaty, T.L.; Shang, J.S. An Innovative Orders-of-Magnitude Approach to AHP-Based Mutli-Criteria Decision Making: Prioritizing Divergent Intangible Humane Acts. *Eur. J. Oper. Res.* **2011**, *214*, 703–715. [CrossRef]
27. Sipahi, S.; Timor, M. The Analytic Hierarchy Process and Analytic Network Process: An Overview of Applications. *Manag. Decis.* **2010**, *48*, 775–808. [CrossRef]
28. Bertol, I.; De Maria, I.C.; Souza, L.S. Manejo e conservação do solo e da água. *Soc. Bras. De Ciência Do Solo* **2019**, *1*, 1355.
29. Saaty, T.L. *The Analytic Hierarchy Process*; McGraw-Hill: New York, NY, USA, 1980.
30. Saaty, T.L. Decision Making with the Analytic Hierarchy Process. *Int. J. Serv. Sci.* **2008**, *1*, 83–98. [CrossRef]
31. Lepsch, I.F.; Espindola, C.R.; Vischi Filho, O.J.; Hernani, L.C.; Siqueira, D.S. *Manual Para Levantamento Utilitário e Classificação de Terras No Sistema de Capacidade de Uso*, 1st ed.; Sociedade Brasileira de Ciência do Solo: Viçosa, MG, Brazil, 2015; Volume 1.
32. EMBRAPA. *Sistema Brasileiro de Classificação de Solos*; EMBRAPA: Brasília, DF, Brazil, 2018.
33. Monteiro, L.I.B.; Pruski, F.F.; Calegario, A.T.; Oliveira, A.N.G.; Pereira, S.B. Methodology for Payment for Ecosystem Services Based on the Concept of Land Use and Management Capability. *Soil. Use Manag.* **2018**, *34*, 515–524. [CrossRef]
34. NASA NASADEM Merged DEM Global 1 Arc Second V001. Available online: https://catalog.data.gov/dataset/nasadem-global-digital-elevation-model (accessed on 4 November 2022).
35. FBDS Permanent Preservation Areas. Available online: http://geo.fbds.org.br (accessed on 8 October 2023).
36. CAR Legal Reserves. Available online: https://www.car.gov.br/#/ (accessed on 8 October 2023).

37. Berlinck, C.N.; Batista, E.K.L. Good Fire, Bad Fire: It Depends on Who Burns. *Flora Morphol. Distrib. Funct. Ecol. Plants* **2020**, *268*, 151610. [CrossRef]
38. Bowman, D.M.J.S.; Balch, J.; Artaxo, P.; Bond, W.J.; Cochrane, M.A.; D'Antonio, C.M.; Defries, R.; Johnston, F.H.; Keeley, J.E.; Krawchuk, M.A.; et al. The Human Dimension of Fire Regimes on Earth. *J. Biogeogr.* **2011**, *38*, 2223–2236. [CrossRef]
39. MapBiomas Método MapBiomas Fogo. Projeto MapBiomas 2021. Available online: https://mapbiomas.org/metodo-mapbiomas-fogo-1 (accessed on 5 October 2023).
40. Borrelli, P.; Robinson, D.A.; Fleischer, L.R.; Lugato, E.; Ballabio, C.; Alewell, C.; Meusburger, K.; Modugno, S.; Schütt, B.; Ferro, V.; et al. An Assessment of the Global Impact of 21st Century Land Use Change on Soil Erosion. *Nat. Commun.* **2017**, *8*, 2013. [CrossRef]
41. Bertoni, J.; Lombardi Neto, F. *Conservação Do Solo*, 10th ed.; Ícone: São Paulo, SP, Brazil, 2017.
42. Cecílio, R.A.; de Oliveira, J.P.B.; de Sousa Teixeira, D.B.; Pruski, F.F.; Zanetti, S.S. Database of Rainfall Erosivity Factor for 141 Locations in Brazil. *Lat. Am. Data Sci.* **2021**, *1*, 95–101. [CrossRef]
43. Durães, M.F.; de Mello, C.R. Spatial Distribution of the Potential and Current Soil Erosion for the Sapucaí River Basin, MG, Brazil. *Eng. Sanit. E Ambient.* **2016**, *21*, 677–685. [CrossRef]
44. Chagas, R.; Morais, S.; Celina, M.; Sales, L. Estimativa Do Potencial Natural de Erosão Dos Solos Da Bacia Hidrográfica Do Alto Gurguéia, Piauí-Brasil, Com Uso de Sistema de Informação Geográfica Estimation of the Natural Soil Erosion Potential of the Upper Gurguéia Basin, Piauí-Brazil, Using Geographic Information System. *Número Espec.* **2017**, *27*, 84. [CrossRef]
45. Salomão, F.X.T. Controle e Prevenção de Processos Erosivos. In *Erosão e Conservação Dos Solos: Conceitos, Temas e Aplicações*; Bertrand Brasil: Rio de Janeiro, RJ, Brazil, 2005.
46. Schaefer, C.E.; Albuquerque, M.A.; Charmelo, L.L.; Campos, J.C.F.; Simas, F.B. Elementos Da Paisagem e a Gestão Da Qualidade Ambiental. *Inf. Agropecuário* **2000**, *21*, 22–44.
47. Resende, M.; Curi, N.; Rezende, S.B.; Silva, S.H.G. *Da Rocha Ao Solo: Enfoque Ambiental*, 1st ed.; UFLA: Lavras, MG, Brazil, 2019.
48. Souza Valladares, G.; da Silva Gomes, A.; Enrique Torresan, F.; Aparecida Gonçalves Rodrigues, C.; Regina Grego, C.; Monitoramento por Satélite, E.; Soldado Passarinho, A. Multicriteria Additive Model in Generating Maps of Susceptibility to Erosion in Rural Area. *Pesqui. Agropecuária Bras.* **2012**, *47*, 1376–1383.
49. ANA. *Balanço Hídrico Quantitativo*; Agência Nacional de Águas e Saneamento Básico: Brasília, DF, Brazil, 2022.
50. Cano-Crespo, A.; Traxl, D.; Thonicke, K. Spatio-Temporal Patterns of Extreme Fires in Amazonian Forests. *Eur. Phys. J. Spec. Top.* **2021**, *230*, 3033–3044. [CrossRef]
51. Ricotta, C.; Bajocco, S.; Guglietta, D.; Conedera, M. Assessing the Influence of Roads on Fire Ignition: Does Land Cover Matter? *Fire* **2018**, *1*, 24. [CrossRef]
52. Syphard, A.D.; Keeley, J.E.; Abatzoglou, J.T. Trends and Drivers of Fire Activity Vary across California Aridland Ecosystems. *J. Arid Environ.* **2017**, *144*, 110–122. [CrossRef]
53. Azevedo, T.; Rosa, M.; Shimbo, J.; Del Lama Marques, C.; Oliveira, M.; Valdiones, A.P.; Teixeira, L.M.S.; Coelho, M. *Relatório Anual Do Desmatamento No Brasil*; MapBiomas: São Paulo, SP, Brazil, 2023.
54. IAS Municípios e Saneamento. Available online: https://www.aguaesaneamento.org.br (accessed on 28 April 2024).
55. Campos, J.A.; da Silva, D.D.; Moreira, M.C.; de Menezes Filho, F.C.M. Environmental Fragility and Land Use Capacity as Instruments of Environmental Planning, Caratinga River Basin, Brazil. *Environ. Earth Sci.* **2021**, *80*, 264. [CrossRef]
56. Cruz, B.B.; Manfré, L.A.; Ricci, D.S.; Brunoro, D.; Appolinario, L.; Quintanilha, J.A. Environmental Fragility Framework for Water Supply Systems: A Case Study in the Paulista Macro Metropolis Area (SE Brazil). *Environ. Earth Sci.* **2017**, *76*, 441. [CrossRef]
57. de Jesus França, L.C.; Lopes, L.F.; de Morais, M.S.; Lisboa, G.D.S.; da Rocha, S.J.S.S.; de Morais Junior, V.T.M.; Santana, R.C.; Mucida, D.P. Environmental Fragility Zoning Using GIS and AHP Modeling: Perspectives for the Conservation of Natural Ecosystems in Brazil. *Conservation* **2022**, *2*, 349–366. [CrossRef]
58. Sahoo, S.; Dhar, A.; Kar, A. Environmental Vulnerability Assessment Using Grey Analytic Hierarchy Process Based Model. *Environ. Impact Assess. Rev.* **2016**, *56*, 145–154. [CrossRef]
59. Nguyen, K.A.; Liou, Y.A. Global Mapping of Eco-Environmental Vulnerability from Human and Nature Disturbances. *Sci. Total Environ.* **2019**, *664*, 995–1004. [CrossRef] [PubMed]
60. Liou, Y.A.; Nguyen, A.K.; Li, M.H. Assessing Spatiotemporal Eco-Environmental Vulnerability by Landsat Data. *Ecol. Indic.* **2017**, *80*, 52–65. [CrossRef]
61. da Fonseca Aguiar, L.; Cataldi, M. Social and Environmental Vulnerability in Southeast Brazil Associated with the South Atlantic Convergence Zone. *Nat. Hazards* **2021**, *109*, 2423–2437. [CrossRef]
62. Malta, F.S.; da Costa, E.M. Socio-Environmental Vulnerability Index: An Application to Rio de Janeiro-Brazil. *Int. J. Public Health* **2021**, *66*, 584308. [CrossRef]
63. Roque, M.P.B.; Ferreira Neto, J.A.; da Cruz Vieira, W.; Rocha, B.D.; Calegario, A.T. Social Vulnerability to Environmental Disasters in the Paraopeba River Basin, Minas Gerais, Brazil. *Nat. Hazards* **2023**, *118*, 1191–1210. [CrossRef]